CARBON TRACERS OF AQUEOUS PROCESSES: ISOTOPIC ANALYSIS OF CR CARBONATE GRAINS WITH IMPLICATIONS FOR BENNU SAMPLES. K. E. Miller[1*], K. Nagashima[2], A. Stevanovic[4], K. Domanik[3], G. R. Huss[2], C. A. Hibbitts[5], C. Phillips-Lander[1], D. Takir[6], K. Bartels[1], M. S. Thompson[7], and M. A. Miller[1], [1]Southwest Research Institute (*kelly.miller@swri.org), [2]University of Hawai'i, [3]University of Arizona, [4]University of Texas, San Antonio, [5]Applied Physics Laboratory, [6]Jacobs, Johnson Space Center, [7]Purdue University.

Introduction: Carbonate grains in carbonaceous chondrites record aqueous alteration events on the asteroidal parent bodies, including evidence for episodic alteration [1], timing of alteration [2-5], and time and temperature evolution of volatiles [5-7]. Spectral features in the 3.4 μm region at asteroid Bennu have been interpreted as coming from carbonate minerals [8, 9]. Coordinated analysis of carbonate grains will be a valuable tool for analysis of Bennu samples, and related analysis of analog materials provides important context for understanding aqueous alteration of carbonaceous asteroids more broadly.

To that end, our team is analyzing carbonates in Bennu analog materials, using Raman spectroscopy to identify carbonates and assess the maturity of related organic materials [10], vacuum reflectance spectroscopy from the ultraviolet through thermal infrared range to constrain contributions from carbonates and organics [11, 12], X-ray microtomography and electron probe microanalysis (EPMA) to assess the distribution of void space, transmission electron microscopy to characterize space weathering effects [13], and EPMA and secondary ion mass spectrometry (SIMS) to measure composition and isotopic ratios. Here, we describe *in situ* analysis of carbon and oxygen isotopes from carbonates in Grosvenor Mountains (GRO) 95577.

Sample: GRO 95577 is a CR1 chondrite, the most altered CR chondrite known to date [14]. It was identified as a spectral analog for Bennu based on the shape and position of the hydration feature as well as similarities in the thermal infrared region [15]. We have analyzed thin section GRO 95577, 61 with a focus on Ca-carbonate grains, which are abundant throughout the thin section. Petrology of the analyzed grains is similar to grains from GRO 95577 shown by [3] and [16]. No rims were identified around carbonate grains.

Method: Ca-carbonate grains were identified in the carbon-coated thin section via EPMA using the Cameca SX-100 at the University of Arizona. Chemical maps of the thin section were acquired, and large, bright spots on the Ca map were examined in further detail via wavelength dispersive spectroscopy (WDS) to verify their composition. Typical diameters for the selected grains were ~50 μm to ensure an appropriate size for isotopic analyses. WDS data confirmed low FeO content for matrix-matching of standards. Prior to SIMS analysis, we marked grains targeted for analysis by removing a small portion of the gold coat with focused ion beam milling with the Zeiss Crossbeam 340 FIB-SEM at the University of Texas at San Antonio.

SIMS analyses of carbon and oxygen isotopes were performed on two successive days on the Cameca ims 1280 ion microprobe at the University of Hawai'i. The UWC3 calcite standard was utilized for both oxygen and carbon to correct instrumental mass fractionation. ^{12}C was measured via Faraday cup (FC), and ^{13}C was measured on the mono-collection electron multiplier (EM). Grains were presputtered prior to analysis to remove any residual carbon coat. Similarly, ^{16}O and ^{18}O were simultaneously measured by two separate FCs, and ^{17}O was resolved from ^{16}OH and measured by mono EM. The grains were subsequently imaged via scanning electron microscope (SEM) to verify that the SIMS pits were fully contained within the FIB fiducials and grain boundaries.

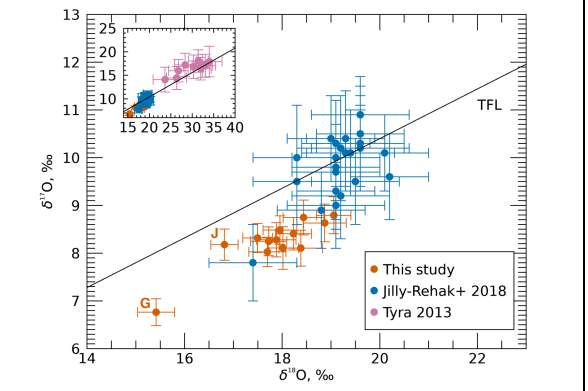

Figure 1. *In situ* oxygen isotopic measurements from GRO 95577. Error bars are 2σ.

Results: Oxygen isotope measurements relative to VSMOW are summarized in Figure 1. Data generally fall in a cluster, with mean values of $\delta^{17}O$ = 8.2±1.0‰ (2σ) and $\delta^{18}O$ = 17.8±1.9‰. Our data are similar to those reported by [17], although our $\delta^{17,18}O$ values are at the lower end of the range they reported. Both datasets were collected in the same laboratory using the same standard and similar methods. Grain G, a sinuous carbonate grain in the matrix, is somewhat enriched in ^{16}O. The neighboring grain Gn falls within the cluster defined by the majority of the measurements. Both

results reported here and those from [17] are enriched in ^{16}O relative to results from [16] (Figure 1 inset).

Our $\delta^{13}C$ data from the same grains are shown relative to PDB in Figure 2**.** The mean value for all data points is $\delta^{13}C = 70.7\pm11.4‰$ (2σ), which overlaps with the bulk value reported by [6] ($\delta^{13}C = 71.1\pm0.4‰$) and is near the top of the range found by [18]. Two discreet ranges are evident in our data (mean $\delta^{13}C = 74.9\pm1.4‰$, n = 6; $\delta^{13}C = 62.9\pm1.8‰$, n = 3) with a single point between the two ranges ($\delta^{13}C = 69.4‰$).

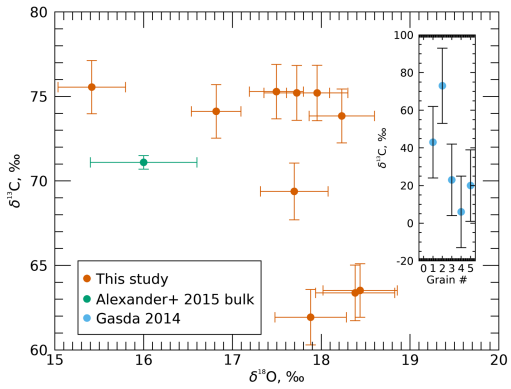

Figure 2. *In situ* carbon isotopic measurements versus $\delta^{18}O$ from GRO 95577, 61. Bulk data from [5] and in situ data from [16] are shown for comparison. Error bars are 2σ.

Discussion: The oxygen isotopic values for individual Ca-carbonate grains are generally similar, but carbon isotope values vary. In the CM chondrites, multiple generations of calcite grains have been identified based on petrologic and oxygen isotopic characteristics [19-22]. Petrologic characteristics (e.g., grain size, composition, morphology, and associated minerals) do not appear to correlate with the $\delta^{13}C$ values measured here. Previous studies have examined $\delta^{13}C$ and $\delta^{18}O$ in chondritic carbonate minerals, but the relationship between these isotopic systems is not currently understood. Based on bulk values, [6] suggested a positive correlation that was interpreted as progressive loss of ^{12}CO or $^{12}CH_4$ gas in an open system with ^{18}O equilibrated with water. In this scenario, higher $\delta^{13}C$ corresponds to later-stage formation. On the other hand, [23] found a negative correlation from bulk measurements attributed to kinetic isotope effects.

[24] reported joint measurements of in situ C and O isotopes from CM chondrites, and found a bimodal distribution in $\delta^{13}C$ and approximately constant $\delta^{17,18}O$, similar to our results for GRO 95577. Based on trace element trends, CL zoning, and oxygen isotopic data, they excluded the possibility that the variable $\delta^{13}C$ represented different carbonate generations, and instead concluded that the values corresponded to formation in diverse microenvironments. These microenvironments may sample different C isotopic reservoirs, such as SOM or IOM [25].

Carbonates in the CR chondrites record a history of aqueous alteration unique from the CM chondrites. Alteration must have begun early after accretion [3]. There is also evidence for alteration 10 Myr or more later, which may have been due to impact heating events [3, 16]. The $\delta^{13}C$ in bulk CR chondrites trends with degree of alteration [6], and if $\delta^{13}C$ is related to the progressive time evolution of the dissolved carbon reservoir with continued alteration then our data suggest the measured grains are late-stage carbonates.

Interestingly, [3] suggest two separate time trends in their Mn-Cr data, but ultimately include all points as a single population on the basis of oxygen isotopic data. Additional measurements of C and Mn-Cr on single grains may help resolve whether the differences we observe in $\delta^{13}C$ are related to alteration progress and time evolution, or sampling of different microenvironments. Coordinated measurements of local porosity and organic maturity near the measured grains may also help resolve the cause of the variation.

Acknowledgments: This project is funded by NASA LARS grant 80NSSC23K0402. We thank the JSC curation team for consultation and for use of this ANSMET meteorite sample.

References: [1] Lee M. R. et al. (2014) *GCA,* 144, 126-156. [2] Jilly C. E. *et al.*, (2014) *MAPS* 49, 2104-2117. [3] Jilly-Rehak C. E. et al. (2017) *GCA,* 201, 224-244. [4] Fujiya W. et al. (2013) *EPSL,* 362, 130-142. [5] McCain K. A. et al. (2023) *Nat. Ast.* 7, 309-317. [6] Alexander C. O. D. et al. (2015) *MAPS,* 50, 810-833. [7] Guo W. and Eiler J. M. (2007) *GCA,* 71, 5565-5575. [8] Kaplan H. *et al.*, (2020) *Science*, 370, eabc3557. [9] Simon A. A. *et al.* (2020) *Science,* 370, eabc3522. [10] Phillips-Lander C. M. et al. (2024) *LPS LV*. [11] Hibbitts C. et al. (2023) *ACM Conference*. [12] Takir D. *et al.*, (2024) *LPS LV,* Abstract #1055. [13] Melendez, L. E., *et al.* (2023) *LPS LIV,* Abstract #2069. [14] Weisberg M. K., Huber H., (2007) *MAPS,* 42, 1495-1503. [15] Hamilton V. *et al.*, (2022) *LPS LIII,* Abstract #1660. [16] Tyra M. A. (2013), *Ph.D. Dissert-ation*. [17] Jilly-Rehak C. E. et al. (2018) *GCA,* 222, 230-252. [18] Gasda P. (2014), *Ph.D. Dissertation*. [19] Tyra M. et al. (2012) *GCA,* 77, 383-395. [20] Tyra M. *et al.*, (2007) *GCA,* 71, 782-795. [21] Lee M. et al. (2013) *GCA,* 121, 452-466. [22] Telus M. et al. (2019) *GCA,* 260, 275-291. [23] Guo W. (2008), *Ph.D. Disser-tation*. [24] Fujiya W. *et al.*, (2015) *GCA,* 161, 101-117. [25] Vacher L. G. et al. (2017) *GCA,* 213, 271-290.